Tetrahedron 64 (2008) 8543–8552

Contents lists available at ScienceDirect

Tetrahedron

journal homepage: www.elsevier.com/locate/tet

Thiol-functionalized shell crosslinked knedel-like (SCK) nanoparticles: a versatile entry for their conjugation with biomacromolecules

Andreas M. Nyström, Karen L. Wooley *

Center for Materials Innovation, Department of Chemistry and Department of Radiology, Washington University in Saint Louis, Saint Louis, MO 63130, USA

ARTICLE INFO

Article history:
Received 4 March 2008
Received in revised form 16 April 2008
Accepted 25 April 2008
Available online 30 April 2008

ABSTRACT

Shell crosslinked knedel-like (SCK) nanoparticles were prepared having thiol-terminated poly(ethylene glycol) (PEG) chains extending throughout their shell layers and were then conjugated with bovine serum albumin (BSA) as a model biomacromolecule. The SCKs originated from amphiphilic block copolymers of acrylic acid and styrene, PAA_{66}-*b*-PS_{71}, pre-functionalized with ca. five mono-*tert*-Boc-protected diamino PEG_{32} per polymer chain, which then had undergone deprotection and amidation with *N*-succinimidyl-*S*-acetylthiohexanionate to introduce an acetyl-protected thiol chain terminus on the end of each PEG graft. Assembly of these amphiphilic graft block copolymers into micelles, by transitioning from *N*,*N*-dimethylformamide to water, was followed by amidation-based crosslinking throughout the shell layer, with the introduction of 2,2′-(ethylenedioxy)-bis(ethylamine) and 1-(3′-dimethylaminopropyl)-3-ethylcarbodiimide methiodide, to afford SCKs bearing the acetyl-protected thiol groups. Deprotection in aqueous buffer solution by reaction with hydroxylamine hydrochloride gave the SCKs presenting a nominal number of ca. 750 thiols per nanoparticle. The solution was assayed by Ellman's method resulting in a concentration of 55±6 μM [HS], theoretical of concentration 58 μM [HS], after which the coupling with BSA was performed immediately. Tetramethylrhodamine-labeled, maleimido-functionalized BSA was allowed to react with the thiol-functionalized SCKs at stoichiometries of ca. 10, 20, and 30 BSAs/SCK, after which UV–vis spectroscopy and Bradford's assay determined a coupling efficiency of >50–60%. The SCK particle diameters were measured by TEM to be 16 nm and 20 nm and their hydrodynamic diameters were measured by dynamic light scattering to be 20 nm and 30 nm, before and after BSA conjugation, respectively.

1. Introduction

One aspect of nanomedicine aims to utilize nano-sized objects, such as micelles and polymeric nanoparticles, for applications as drug delivery vehicles and diagnostic agents, with the ultimate goal of treating diseases with better selectivity and outcome.[1–5] Increasing the bioavailability of a therapeutic, utilization of polyvalent interactions for tissue-specific binding, and high contrast imaging are features that are being made possible by using nanoparticle-based platforms.[2–7] From a medical, biological, and chemical perspective, nanomedical agents are complex systems to design. One key challenge for the successful application of nano-objects in medicine is to achieve tissue-specific targeting in vivo.[3,5] Targeting moieties, ranging in size from small molecules and peptides to larger protein and antibody targeting components, have been explored recently for a range of applications.[3,5] For a given target, it is often necessary to screen several types of targeting components for a given nanocarrier system.[5] This systematic evaluation requires robust chemistry that allows for high coupling efficiency, since the targeting components are often prepared in small scale at a high cost.

Shell crosslinked knedel-like (SCK) nanoparticles are an attractive platform to explore for a range of nanomedical applications.[8–10] SCKs are derived from polymeric micelles assembled in aqueous solution from amphiphilic block copolymers; these micelles are then crosslinked throughout the shell domain.[11,12] The introduction of covalent crosslinks within the nanostructures provides stabilization of the structure, thereby circumventing limitations that the critical micelle concentration (CMC) imposes on polymeric micelle assemblies for in vivo applications.[9,13]

Typically, SCKs have been conjugated with small molecules and peptides through standard amidation chemistry with the acrylic acid residues of the parent polymer prior to self assembly or by the post-functionalization of the preformed SCKs in solution.[14–20] The pre-functionalization strategy[16,17] has been employed successfully for small molecule conjugation, but is not applicable for conjugation of larger biomacromolecules, since these are expected to hinder the self-assembly process. Post-functionalization of SCKs in

* Corresponding author. Tel.: +1 314 935 7136; fax: +1 314 935 9844.
E-mail address: klwooley@artsci.wustl.edu (K.L. Wooley).

0040-4020/$ – see front matter © 2008 Elsevier Ltd. All rights reserved.
doi:10.1016/j.tet.2008.04.104

solution also typically utilizes acrylic acid residues in the shell domain of the nanoparticle for activated ester-type couplings to primary amines of the targeting component.[14,15,18–20] However, this type of coupling chemistry is limited to small molecules and peptides, for which the location of an amine can be engineered easily. Proteins carry a multitude of primary amines, typically, and in the case of antibodies coupling via the amines in the active FAB region of an antibody may result in a loss of bioactivity and targeting.[21] Indeed, we have preliminary results indicating that such a loss of activity can occur when preparing SCK–antibody conjugates via activated ester methodologies.[22]

Since antibodies and proteins are promising targeting moieties for directing nanoscale agents for drug delivery and imaging, we opted to develop a new type of functional SCK nanoparticle that carries protected thiol groups on a grafted poly(ethylene glycol) (PEG) spacer.[23] In this case, the PEG spacer is also expected to improve the in vivo biodistribution of the SCK nanoparticles.[16,20,24] The thiol group is an attractive functionality to have on nanoparticles since reversibly linked bioconjugates can be prepared by disulfide formation, which may allow for reductive release of a targeting or therapeutic component.[23,25–36] In addition, thiol-maleimide based couplings are known to proceed efficiently in solution,[23,29,30] and the protocol for conjugation of larger biomacromolcules such as enzymes with proteins via this methodology is well established in the literature.[30] Also, site-specific attachment of maleimdio groups on the Fc region of antibodies have been developed[30] and successfully utilized for the preparation of dendrimer–antibody[37] and micellar–antibody conjugates.[38] Given the instability of the maleimide functionality in solution at physiological pH,[39] it is more beneficial to incorporate this functionality on the biomacromolecule as opposed to the nanoparticle, because the particle requires several steps of purification in aqueous solution by dialysis over a longer period of time.

In this study, we describe the preparation of polymer precursors based on block copolymers of poly(acrylic acid) and polystyrene, grafted with PEG carrying protected SH groups in the ω-terminus, and the self assembly of these polymers into micelles and SCK nanoparticles. These functional nanoparticles were then conjugated with a model protein, bovine serum albumin (BSA), creating SCK–protein conjugates with high coupling efficiency. The particle–protein conjugates were analyzed by biochemical assays, dynamic light scattering (DLS), and transmission electron microscopy (TEM), among other techniques.

2. Results and discussion

2.1. Preparation of the polymers

The amphiphilic block copolymer used in this study was synthesized in a three-step procedure. First, *tert*-butyl acrylate (*t*-BA) was polymerized by using reversible addition–fragmentation chain transfer polymerization (RAFT) with *S*-1-dodecyl-*S*′-(α,α′-dimethyl-α″-acetic acid)trithiocarbonate (DDMAT) as chain transfer agent (CTA), **2**, to form polymer **4**. Compared with other CTAs, DDMAT has the advantage of easier handling (solid) and having less of an unfavorable odor. The P*t*BA macrochain transfer agent was then chain extended with styrene to form the diblock copolymer P*t*BA-*b*-PS **5**. As depicted in Figure 1 and summarized in Table 1 (entries 1 and 2), polymers **4** and **5** showed unimodal and narrow molecular weight distributions (polydispersity indices (PDI)<1.2), indicating control over the copolymerization process. As a last step, the *tert*-butyl groups of the block copolymer were removed by acidolysis in TFA/CH_2Cl_2 to yield the amphiphilic block copolymer **6**.

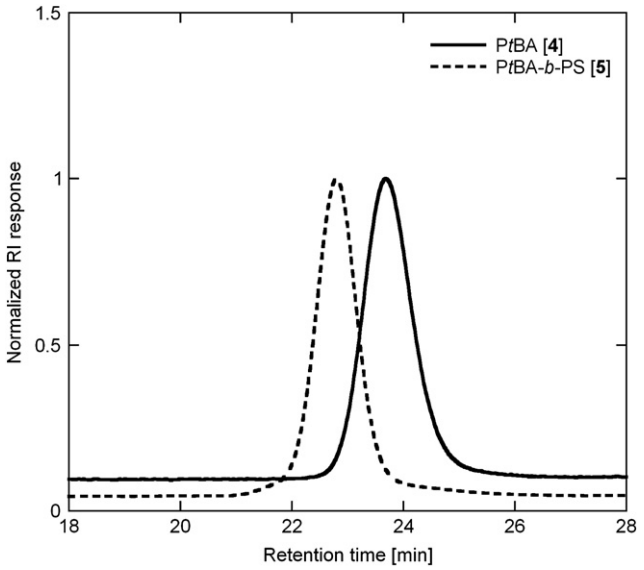

Figure 1. GPC traces for polymers **4** and **5**.

The PAA-*b*-PS block copolymer was then further functionalized with a mono protected poly(ethylene glycol) (PEG), utilizing standard amidation chemistry in DMF to yield polymer **8**, PAA-*g*-(Boc–NH–PEG)-*b*-PS, carrying an average of five PEG chains per polymer chain (Scheme 1 and Fig. 2, upper panel).[17] The Boc-groups of this polymer were subsequently removed by acidolysis with TFA. The polymer was purified by extensive dialysis and, finally, was lyophilized to yield polymer **11**. As a last step, methylester-protected sulfohydryl groups were introduced at the NH_2 groups of the PEG spacer by reaction with SATH, **1**, to form polymer **13**.

A similar synthetic pathway was used for the preparation of the amphiphilic block copolymer that carries chelators for ^{64}Cu radiolabeling, which can be used for in vivo PET imaging.[16,17,20] The synthesis began with the introduction of Boc-protected DOTA having a short lysine spacer to form polymer **9** with an average of five DOTA groups per polymer chain (Scheme 2 and Fig. 2, lower panel).[17] Polymer **9** was then further reacted with the monoBoc-

Table 1
Summary of polymers prepared

Sample	Polymer	PEG	DOTA	–$SCOCH_3$	M_n [Da]	M_n [Da]	M_w [Da]	PDI
					^{1}H NMR	GPC	GPC	GPC
4	P*t*BA	—	—	—	8700	6400	7000	1.09
5	P*t*BA-*b*-PS	—	—	—	16,100	11,000	11,700	1.10
6	PAA-*b*-PS	—	—	—	12,500	—[a]	—[a]	—[a]
8	PAA-*g*-(CONH–PEG–NH–Boc)-*b*-PS	5	—	—	21,000	—[a]	—[a]	—[a]
9	PAA-*g*-(CONH–lysine–DOTA–Boc)-*b*-PS	—	5	—	17,700	—[a]	—[a]	—[a]
10	PAA-*g*-(CONH–lysine–DOTA–Boc)-*g*-(CONH–PEG–NH–Boc)-*b*-PS	4	5	—	23,900	—[a]	—[a]	—[a]
11	PAA-*g*-(CONH–PEG–NH_2)-*b*-PS	5	—	—	20,500	—[a]	—[a]	—[a]
12	PAA-*g*-(CONH–lysine–DOTA–COOH)-*g*-(CONH–PEG–NH_2)-*b*-PS	4	5	—	23,500	—[a]	—[a]	—[a]
13	PAA-*g*-(CONH–PEG–NHCO–C_5H_{10}–$SCOCH_3$)-*b*-PS	5	—	5	21,300	—[a]	—[a]	—[a]
14	PAA-*g*-(CONH–lysine–DOTA–COOH)-*g*-(CONH–PEG–NHCO–C_5H_{10}–$SCOCH_3$)-*b*-PS	4	5	4	24,300	—[a]	—[a]	—[a]

[a] The PAA-containing polymers could not undergo evaluation by GPC using THF as the eluent, due to adsorption onto the column packing material.

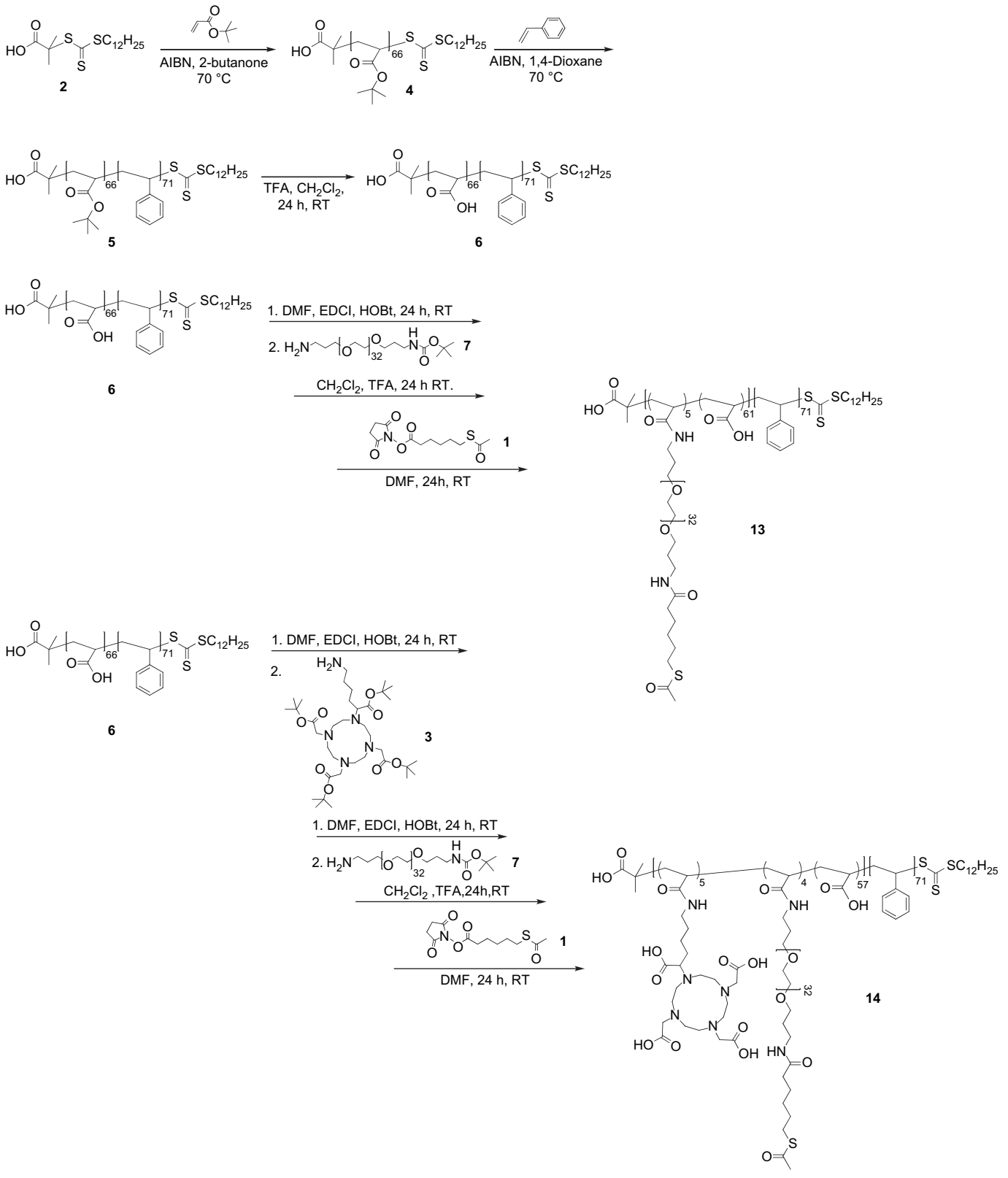

Scheme 1. Synthesis of the functional graft block copolymers **13** and **14**.

protected PEG, followed by deprotection upon reaction with TFA and coupling with SATH, **1**, to form polymer **14**, loaded with DOTA and protected thiol groups connected through PEG spacers. Figure 2 depicts the proton NMR (500 MHz) spectrum of polymer **8** (upper panel) in DMSO-d_6 and polymer **9** (lower panel) in DMF-d_7. The degree of attachment of the PEG was calculated from the integrals corresponding to the styrene unit protons *j* (6.48–7.31 ppm), and the integrals corresponding to the PEG protons *h* (3.41–3.52 ppm).[16,17] The degree of DOTA–lysine attachment was calculated in a similar fashion, by using the signal arising from styrene

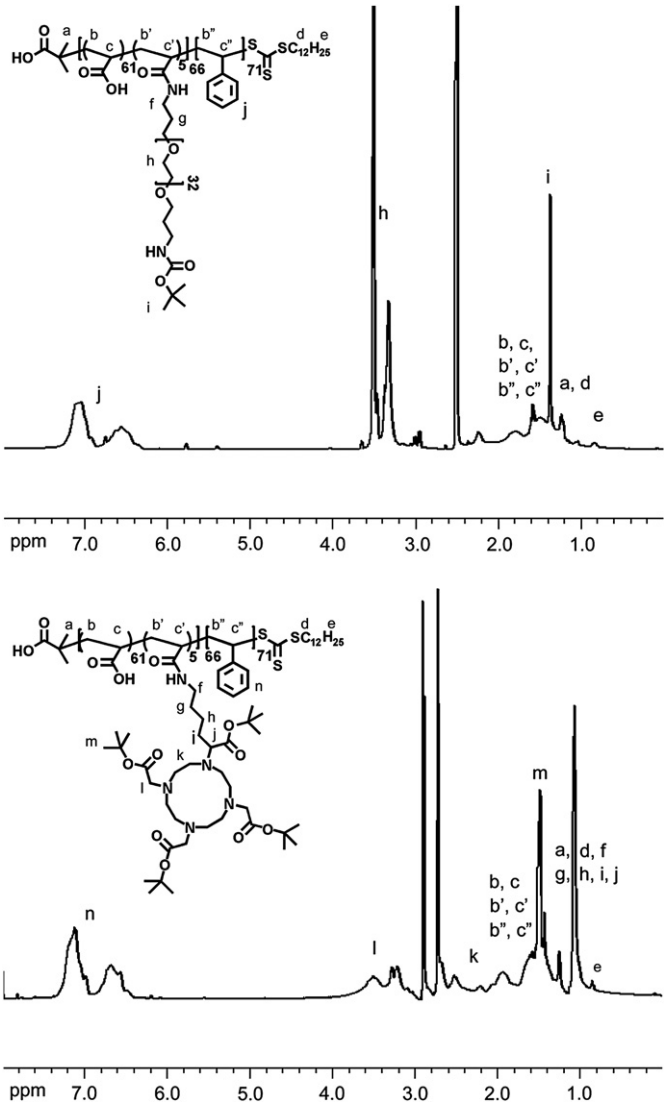

Figure 2. ^{1}H NMR spectra (500 MHz) collected in DMF-d_7 for the polymers **8** and **9** in the upper and lower panels, respectively.

protons *n* (6.49–7.32 ppm), and the intensities of **l** and **k** from the DOTA unit protons.[16,17]

2.2. Preparation of the SCKs

As depicted in Scheme 2, micelles from the block copolymers **13** and **14** were prepared by following the pre-established protocol described in Section 4. The block copolymers were dissolved in DMF at a concentration of 1 mg mL^{-1}. Self assembly was induced by addition of an equal amount of water over the course of 3 h. The micelles were transferred to dialysis tubing and dialyzed for 4 days. The SCKs were obtained by crosslinking of the hydrophilic shell layer through condensation of approximately 50% of the carboxylic acid functionalities of the PAA chain segments with the amine groups of crosslinker (2,2′-(ethylenedioxy) bis(ethylamine)), followed by extensive dialysis against buffer to remove the small molecule by-products.[†] While preparing SCKs from micelle **16**, we

[†] The reported percentages of crosslinking are the stoichiometries of amine crosslinker added to the carboxylic acid groups in the polymer. These values are, therefore, the maximum amounts of crosslinking that could have occurred, rather than the true extents of crosslinking.

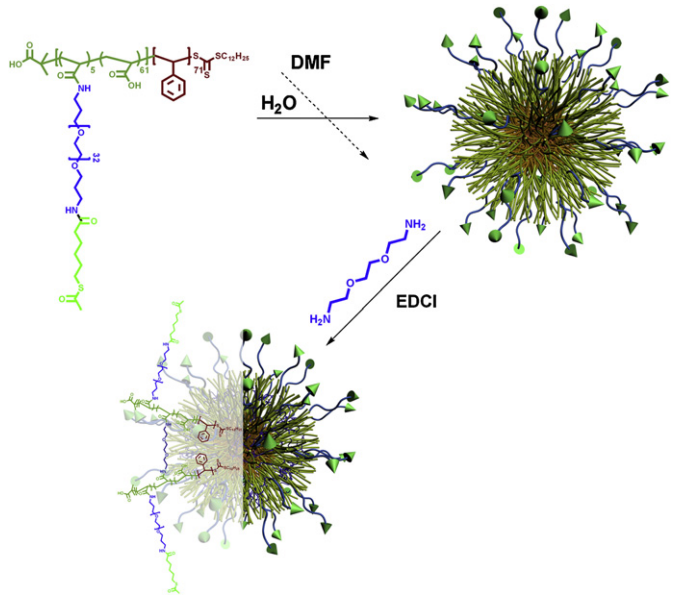

Scheme 2. Preparation of the micelles and SCKs.

found that the micelle carrying five DOTA units per polymer chain was not storage-stable in solution and precipitated over time. We have encountered similar problems previously with polymers having more than three or four DOTA groups per polymer chain. This instability prohibited accurate AFM and TEM analysis of the micelle, and we could proceed no further with this micelle.

2.3. Characterization of the SCKs

The shape and size of the micelles **15** and SCKs **17** were investigated by TEM, DLS, and AFM. The results of these characterizations are summarized in Table 2. TEM analysis showed that the size of the micelles **15** was ca. 18 nm and that of SCKs **17** was ca. 16 nm. Figure 3 depicts the TEM images of the micelle **15** (a) and SCK **17** (b), obtained from the block copolymer **13**. Dynamic light scattering analysis of these samples revealed that the hydrodynamic diameters of the micelles and SCKs in aqueous medium were larger than were the TEM-measured diameters, because the PAA shells were hydrated and, consequently, swelled under the hydrated state. Both the micelle **15** and SCK **17** were in the size range of 21 nm by DLS. AFM imaging on mica was also employed to characterize the micelles and SCKs. The upper and lower panels of Figure 4 show the heights of the micelle **15** and SCK **17**, respectively, indicating that crosslinking of micelle **15** to SCK **17** resulted in a small height decrease from 18 nm to 14 nm.

2.4. Preparation of the conjugates

The objective of attaching protected sulfohydryl groups on a short PEG spacer on the SCKs was to create surface functional nanoparticles that could be conjugated with maleimdo functional small molecules and/or larger biomacromolecules, such as proteins and antibodies, for further use as targeting entities for in vivo imaging and tissue-specific drug delivery. Previously published work from our group has indicated that grafting PEG chains is an effective method for increasing blood circulation time of SCK nanoparticles.[16,17] The methylester protecting groups on the SH-functionality on the PEG spacer were designed to be removed by treatment with hydroxylamine according to standard protocols to yield SH groups available for conjugation.[30] The remaining –SH groups after an initial conjugation could then be used for further

Table 2
Summary of micelles, SCKs, and SCK–BSA conjugates prepared

Sample	H_{av} [nm] AFM	$(D_h)_n$ [nm] DLS	D_{av} [nm] TEM	[SH μM] Theoretical	[SH μM] Ellmans	BSA [μg mL^{-1}] Theoretical	BSA [μg mL^{-1}] UV–vis	BSA [μg mL^{-1}] Bradford
15	18±2	21±2	18±3	—	—	—	—	—
17	14±2	21±5	16±3	—	nd	—	—	—
18	—	—	—	58	55±6	—	—	—
19	—	2.2±0.7	—	—	—	—	—	—
20	—	31±3	20±3	—	—	32	~6	20±8
21	—	32±5	20±2	—	—	64	43	37±8
22	—	28±3	20±2	—	—	119	81	85±8

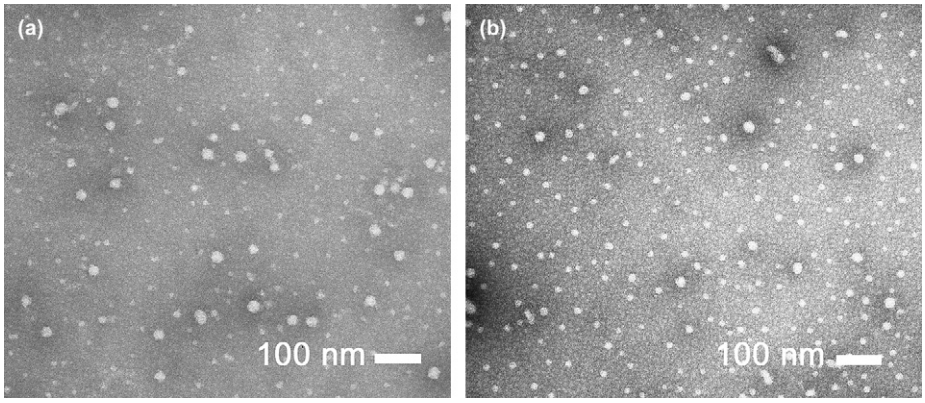

Figure 3. TEM images of micelle **15** (a) and SCK **17** (b).

conjugation protocols or could be capped, in order to prevent particle–particle reactions (Scheme 3).

The prepared SCK solution **17** was deprotected by reaction with 0.5 M hydroxylamine for 3 h in buffer (100 mM PBS, 0.1 M NaCl, 10 mM EDTA, pH 7.4) to yield SCK **18**.[30] A large excess of hydroxylamine was employed to account for potential difficulties in performing the deprotection on a large polyvalent nanostructure. The solution was immediately assayed by Ellman's[40] method to assess the concentration of SH groups in solution. These deprotected SCKs were then subjected to conjugation with the complementary, maleimido-functionalized BSA. Table 2 summarizes the results of the conjugation reactions and the assay results. SCK **18** had an SH concentration of 55±6 μM, which is very close to the theoretical concentration of 58 μM, indicating good cleavage of the protecting group. Ellman's assay of SCK **17** before cleavage of the protective group resulted in undetectably low concentration of SH groups. Solutions of SCK **18** were conjugated to various ratios of tetramethylrhodamine-labeled BSA **19**, carrying malemido groups for conjugation to form SCKs **20**–**22**. The reaction was allowed to proceed for 6 h, after which an excess of ethyl maleimide was added to the reaction to cap any remaining free SH groups.[41] After 16 h of stirring at room temperature, the reaction mixtures were transferred to dialysis tubing and dialyzed against buffer for 7 days to remove unconjugated BSA. In this case, dialysis tubing having a MWCO of 100 kDa was employed and a control dialysis of BSA was performed in parallel. The control dialysis verified that >85% of the free BSA was removed during the dialysis process. The chromophore attached to the BSA allowed for a direct characterization of the BSA concentration by UV–vis spectroscopy. In addition, Bradford assays[42] were performed to quantify the protein concentration in solution by an indirect method.

Figure 5 shows the UV–vis analysis of the prepared conjugates, where an increasing absorption at 550 nm with increasing BSA

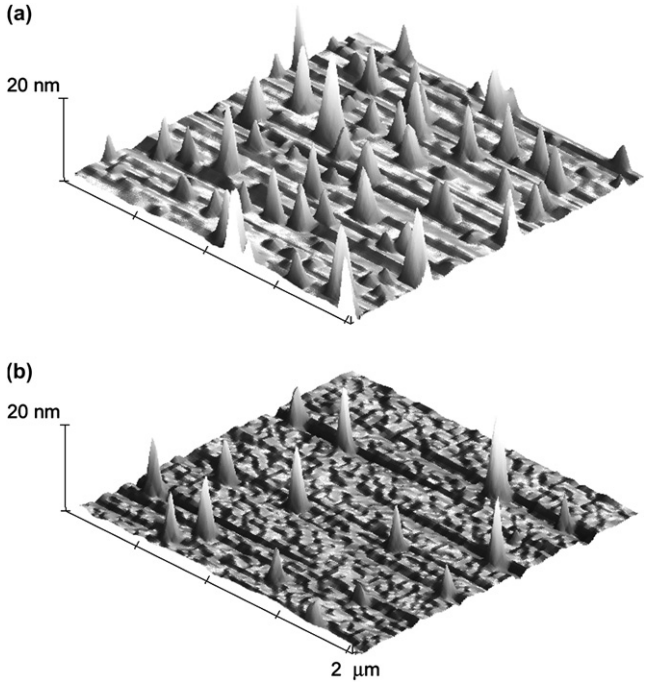

Figure 4. AFM images of micelle **15** (a) and SCK **17** (b).

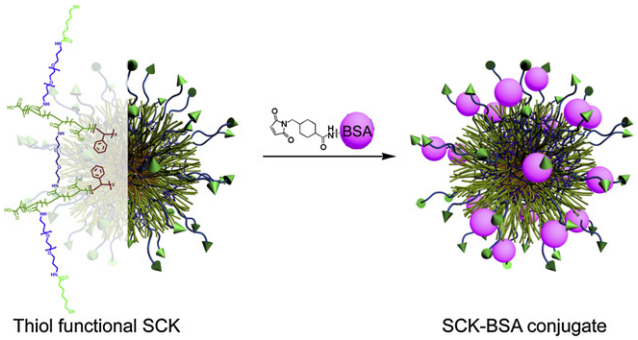

Scheme 3. Conjugation of thiol-functionalized SCKs with maleimido-functionalized and tetramethylrhodamine-labeled BSA.

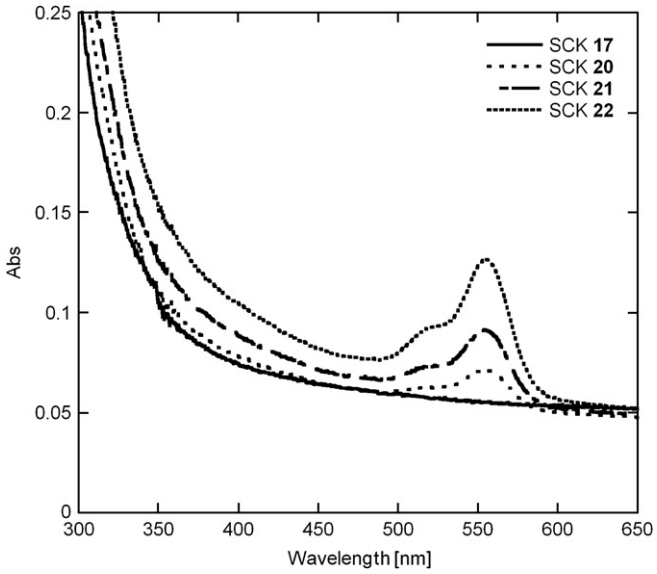

Figure 5. UV–vis spectra of the SCK **17** and SCK–BSA conjugates **20**–**22**.

concentration can be observed. In the case of SCK **20**, the BSA concentration was too low to accurately quantify from our calibration curve. For SCK **21** and **22** the absorptions correspond to BSA concentrations of 43 μM and 81 μM, close to the theoretical of 64 μM and 119 μM, respectively. This corresponds to a coupling efficiency in the range of 50–60% (when accounting for removal of only 85% of any free BSA). The SCK–BSA conjugates were also analyzed using the Bradford assay (calibrated with BSA standards),[42] with comparable results.

The SCK–BSA conjugates were analyzed by TEM and DLS. Figure 6 shows the TEM images of SCK–BSA conjugates **21** (a), and **22** (b). For all conjugations based on SCK **17**, the sizes were determined to be ca. 20 nm in diameter. It is expected that attaching a small number (~10, ~20, and ~30 nominal units per SCK) of BSA to the SCK structure should only increase the overall diameter of the nanoparticle slightly, since BSA is small, relative to the SCK. In the TEM images of the conjugates prepared, a portion of wormlike structures can be distinguished for the conjugates **20**, **21**, and **22**. Such structures could be a result of either particle–particle reactions such as disulfide formation during prolonged reaction times, or aggregation of particles due to protein–protein and/or protein–particle interactions.

The conjugates were analyzed by DLS to assess their hydrodynamic diameters in solution, and the results are summarized in Table 2. The DLS experiments showed that the sizes of the nanoparticles in solution increased from ca. 20 nm to ca. 30 nm after conjugation. In several of the DLS runs, the volume-averaged hydrodynamic diameter distribution was bimodal and contained a minor component of larger structures (80–120 nm) that contribute to an increase in average diameter (see Supplementary data). Since the increase in diameter of the nanoparticle when conjugating a small protein should be very small, we attribute the increase of the nanoparticle diameter to the presence of the wormlike structures that could be seen by TEM analysis. The presence of free BSA (with a size of 2.2 nm in solution) could not be detected in any of the samples by DLS, and is most likely too small to be imaged by TEM at these magnifications.

3. Conclusions

A new type of thiol-functionalized SCK nanoparticle has been developed. The SCK carrries multiple masked SH groups extended upon a grafted PEG spacer that can be unmasked by a standard deprotection reaction with hydroxylamine in aqueous solution. The activation of the SH group could be quantified by standard assays, and the SCK nanoparticle was successfully conjugated with different ratios of BSA as a model protein through maleimide-thio mediated reactions with good coupling (>50%) efficiency. The successful attachment and high coupling efficiency of BSA to the nanoparticle was demonstrated by biochemical assays, dynamic light scattering, and UV–vis spectroscopy. In the case of the SCK nanoparticle carrying DOTA chelators for ^{64}Cu PET imaging, we encountered precipitation of the polymer micelle that will require further optimization of the polymer precursor before we can proceed with assessing the biodistribution of these nanoparticles. In parallel with this work, mixed micelle preparation techniques will be pursued in an effort to further optimize the conjugation of peptides, proteins, and antibodies both through disulfide linkages and thio-maleimide based couplings. Considering the cost of antibodies and peptides intended for in vivo targeting, a high coupling efficiency is a prerequisite, and can be obtained by this methodology. This work is the first step to develop SCK nanoparticles for these types of couplings, and when further optimized, offers a possibility to screen a multitude of targeting components for a given nanoscale platform utilizing efficient and reliable conjugation chemistry that, thus far, has been achieved with mixed results using activated ester based couplings.

4. Experimental

4.1. Instrumentation

UV–vis spectra were acquired on a Varian Cary 1E UV–vis system (Varian, Inc., Palo Alto, CA) using PMMA cuvettes. ^{1}H NMR spectra were recorded at 300 or 500 MHz as solutions in $CDCl_3$,

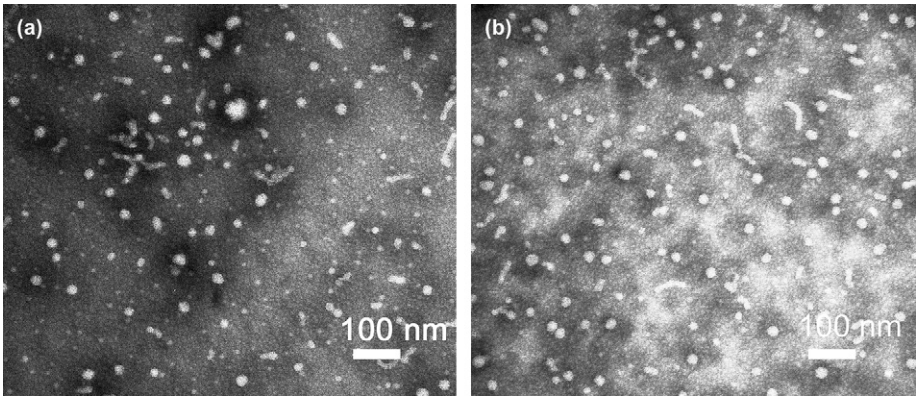

Figure 6. TEM images of SCK–BSA conjugates **21** (a) and **22** (b).

CD_2Cl_2, CD_2Cl_2-TFA-*d*, or DMF-d_7 on a Varian Unity-plus 300 or Varian Inova 500 spectrometer, respectively, with the solvent proton signal as internal standard. Gel permeation chromatography (GPC) was conducted on a Waters 1515 HPLC (Waters Chromatography, Inc.) equipped with a Waters 2414 differential refractometer, and a three-column series PL_{gel} 5 μm Mixed C, 500 Å, and 10^4 Å, 300×7.5 mm columns (Polymer Laboratories, Inc.). The system was equilibrated at 35 °C in THF, which served as the polymer solvent and eluent with a flow rate of 1.0 mL min^{-1}. Polymer solutions were prepared at a known concentration (ca. 1–3 mg mL^{-1}) and an injection volume of 100 μL was used. Data collection and analysis were performed, respectively, with Precision Acquire software and Discovery 32 software (Precision Detectors, Inc.). The height measurements (H_{av}) and distributions for the SCKs were determined by tapping-mode atomic force microscopy (AFM) under ambient conditions in air. The AFM instrumentation consisted of a Nanoscope III BioScope system (Digital Instruments, Veeco Metrology Group; Santa Barbara, CA) and standard silicon tips (type, OTESPA-70; *L*, 160 μm; normal spring constant, 50 N m^{-1}; resonance frequency, 246–282 kHz). The sample solutions were either spin cast from native concentration, or drop (50–100 μL) deposited onto freshly cleaved mica and allowed to settle freely for 30 s, after which the excess solution was removed by a filter paper and the mica surface was allowed to dry in air. Samples for transmission electron microscopy (TEM) measurements were diluted with a 1% phosphotungstic acid (PTA) stain (v/v, 1:1). Carbon grids were exposed to oxygen plasma treatment to increase the surface hydrophilicity. Micrographs were collected at 100,000× magnification and calibrated using a 41 nm polyacrylamide bead from NIST. The number-average particle diameters (D_{av}) and standard deviations were generated from the analysis of particles from at least two different micrographs. Hydrodynamic diameters (D_h) and distributions for the SCKs in aqueous solutions were determined by dynamic light scattering (DLS). The DLS instrumentation consisted of a Brookhaven Instruments Limited (Worcestershire, UK) system, including a model BI-200SM goniometer, a model BI-9000AT digital correlator, a model EMI-9865 photomultiplier, and a model 95-2 Ar ion laser (Lexel, Corp.; Farmindale, NY) operated at 514.5 nm. Measurements were made at 25±1 °C. Prior to analysis, solutions were filtered through a 0.45 μm Nylon filter, and centrifuged in a model 5414 microfuge (Brinkman Instruments, Inc.; Westbury, NY) for 4 min to remove dust particles. Scattered light was collected at a fixed angle of 90°. The digital correlator was operated with 522 ratio spaced channels and initial delay of 0.1 μs, a final delay of 5.0 μs, and a duration of 8 min. A photomulitplier aperture of 200 μm was used, and the incident laser intensity was adjusted to obtain a photon counting of 200 kcps. Only measurements in which the measured and calculated baselines of the intensity autocorrelation function agreed to within 0.1% were used to calculate particle size. Particle size distributions were performed with the ISDA software package (Brookhaven Instruments Company), which employed single-exponential fitting, cumulants analysis, and non-negatively constrained least-squares particle size distribution analysis routines.

4.2. Materials

Polymerizations were performed on a double manifold (0.1 mmHg vacuum, 99.99% N_2), with glassware and syringes that were dried in an oven (100 °C) for at least 1 h, and with syringes that were washed with N_2 (3×), prior to use. Styrene (99%), and *tert*-butyl acrylate (*t*-BA, 99%) were received from Sigma–Aldrich Company (St. Louis, MO) and distilled from calcium hydride, and stored under N_2 prior to use. Trifluoroacetic acid (TFA; 95%; Aldrich), 2,2′-(ethylenedioxy)-bis(ethylamine) (97%; Aldrich), 1-(3′-dimethylaminopropyl)-3-ethylcarbodiimide methiodide (EDCI; 98%; Aldrich), NH_2–PEG–NH_2 (Aldrich), and tetramethylrhodamine functional BSA (Aldrich) were used as received. Sulfosuccinimidyl-4-(*N*-maleimidomethyl) cyclohexane-1-carboxylate (Sulfo-SMCC), Commassie Plus (Bradford) assay kit, 2,4,6,-trinitrobenzene sulfonic acid (TNBS), Ellman's reagent, and Zeba desalting columns were obtained from Pierce. *N*-Succinimidyl-*S*-acetylthiohexanionate (SATH) (**1**),[43] (*S*-1-dodecyl-*S*′-(α,α′-dimethyl-α″-acetic acid)trithiocarbonate) (DDMAT) (**2**),[44] and Boc-protected DOTA–lysine (**3**)[16,17] were synthesized as reported previously. Spectra/Por membrane tubes were purchased from Spectrum Medical Industries, Inc. and were used for dialysis. Nanopure water (18 MΩ cm) was acquired by means of a Milli-Q water filtration system (Millipore Corp.). All other reagents were obtained from Sigma–Aldirch and used as received. Flash column chromatography was performed using 32–63 D 60 Å silica gel from ICN SiliTech (ICN Biomedicals GmbH, Eschwege, Germany). Ellman's assay calibration curve was constructed using cysteine in aqueous buffer (100 mM PBS, 0.1 M NaCl, 10 mM EDTA, pH 7.4) at 412 nm.[40] TNBS assay calibration curve was constructed using lysine in aqueous buffer (0.1 M $NaHCO_3$ buffer, pH 8.3) at 335 nm.[45,46] Commaisse plus (Bradford) assay calibration curves were constructed using BSA in aqueous buffer (5 mM PBS, 5 mM NaCl, pH 7.4) at 595 nm.[42] Absorption–concentration plots for tetramethylrhodamine functional BSA were constructed in aqueous buffer (5 mM PBS, 5 mM NaCl, pH 7.4) at 595 nm and 550 nm.

4.3. Synthesis

*4.3.1. Preparation of the PtBA (**4**)*

A flame-dried 50 mL Schlenk flask equipped with a magnetic stir bar was charged with DDMAT **2** (0.28 g, 0.78 mmol), *t*-BA (10.0 g, 78.1 mmol), AIBN (6.4 mg, 39 μmol), and 2-butanone (10.0 g, 139 mmol). The flask was sealed with a rubber septum and stirred for 10 min at room temperature to ensure a homogeneous mixing. The reaction mixture was degassed by several freeze–pump–thaw cycles (>3), after which the flask was allowed to return to room temperature and was stirred for an additional 10 min. The flask was then immersed into a pre-heated oil bath at 70 °C to start the polymerization. The polymerization was monitored by analyzing aliquots collected at pre-determined times by ^{1}H NMR spectroscopy. As the expected monomer conversion was reached, after ca. 2 h, the polymerization was quenched by quick immersion of the reaction flask into liquid N_2. THF (15 mL) was added to the reaction flask and the polymer was purified by precipitation into 2 L of a methanol/ice mixture thrice. The precipitants were collected and dried under vacuum overnight to afford **4** (5.5 g, yield 91%, conversion 60%) as a yellow powder. ^{1}H NMR: M_n=8700 Da. GPC: M_n=6400 Da, M_w=7000 Da, PDI=1.09. ^{1}H NMR ($CDCl_3$): δ 0.87 (m, CH_3CH_2–), 1.20–1.85 (br, –$CHCH_2$– of the polymer backbone, alkyl chain of initiator, and HOOCC(CH_3)$_2$–), 1.30–1.61 (br, CH_3C), 2.13–2.38 (br, –$CHCH_2$– of the polymer backbone), 3.25–3.38 (br, –SCSCH_2–), 4.62–4.72 (br, –CH_2CHS) ppm.

*4.3.2. Preparation of PtBA-b-PS (**5**)*

A flame-dried 50 mL Schlenk flask equipped with a magnetic stir bar was charged with P*t*BA **4** (4.0 g, 0.46 mmol), styrene (9.56 g, 91.9 mmol), AIBN (3.8 mg, 23 μmol), and 1,4-dioxane (9.56 g, 109 mmol). The flask was sealed with a rubber septum and stirred for 10 min at room temperature to ensure a homogeneous mixing. The reaction mixture was degassed by several freeze–pump–thaw cycles (>3), after which the flask was allowed to return to room temperature and was stirred for an additional 10 min. The flask was then immersed into a pre-heated oil bath at 60 °C to start the polymerization. The polymerization was monitored by analyzing aliquots collected at pre-determined times by ^{1}H NMR spectroscopy. As the expected monomer conversion was reached, after ca. 38 h, the polymerization was quenched by quick immersion of the

reaction flask into liquid N_2. THF (15 mL) was added to the reaction flask and the polymer was purified by precipitation into 2 L of a methanol thrice. The precipitants were collected and dried under vacuum overnight to afford **5** (5.3 g, yield 74%, conversion 33%) as a yellow powder. ^{1}H NMR: M_n=16,100 Da. GPC: M_n=11,000 Da, M_w=11,700 Da, PDI=1.10. ^{1}H NMR ($CDCl_3$): δ 0.87 (m, CH_3CH$_2$–), 1.20–1.85 (br, –CHCH_2– of the polymer backbone, alkyl chain of initiator, and HOOCC(CH_3)$_2$–), 1.30–1.61 (br, CH_3C), 2.13–2.38 (br, –CHCH$_2$– of the polymer backbone), 3.25–3.38 (br, –SCSCH_2–), 4.62–4.72 (br, –CH$_2$CHS), 6.32–7.21 (br, *Ar–H*) ppm.

*4.3.3. Preparation of PAA-b-PS (**6**): general procedure for TFA deprotection of the polymers*

A flame-dried 100 mL round bottom flask equipped with a magnetic stir bar was charged with P*t*BA-*b*-PS **5** (4.8 g, 300 μmol) and 50 mL of dichloromethane (50 mL). TFA (30 mL) was added to the stirred solution and the reaction mixture was stirred for 20 h at room temperature, after which the solvent was removed under vacuum. The crude product was resuspended in THF (15 mL) and transferred to a presoaked dialysis tubing (MWCO ca. 6000–8000 Da), and dialyzed against nanopure H_2O for 4 days, to remove all of the impurities, after which the solution was lyophilized to yield polymer **6** as a yellowish solid (3.68 g, 97%). ^{1}H NMR: M_n=12,500 Da. ^{1}H NMR ($CDCl_3$+0.05% TFA-d_1): δ 0.85 (m, CH_3CH$_2$–), 1.21–1.87 (br, –CHCH_2– of the polymer backbone, alkyl chain of initiator, and HOOCC(CH_3)$_2$–), 2.10–2.41 (br, –CHCH$_2$– of the polymer backbone), 3.22–3.36 (br, –SCSCH_2–), 4.61–4.73 (br, –CH$_2$CHS), 6.31–7.27 (br, *Ar–H*) ppm.

*4.3.4. Preparation Boc–NH–PEG–NH$_2$ (**7**)*

A flame-dried 50 mL round bottom flask equipped with a magnetic stir bar was charged with 1.5 kDa diamino PEG (4.3 g, 2.9 mmol), 4-dimethylaminopyridine (105 mg, 0.86 mmol), triethyl amine (870 mg, 8.61 mmol), and 25 mL of CH_2Cl_2. The solution was stirred at 0 °C and Boc-anhydride (0.751 mg, 3.44 mmol) in 2 mL of CH_2Cl_2 was added to the reaction mixture. The reaction mixture was stirred for 20 h, after which the solution was concentrated under vacuum, resuspended in 10 mL of CH_2Cl_2 and the polymer was purified by precipitation at −10 °C into 150 mL of a diethyl ether/hexane mixture (3:1) thrice. The precipitants were collected by centrifugation and washed with additional cold diethyl ether and finally dried under vacuum. The polymer was further purified by flash chromatography on silica gel eluting with 500 mL of CH_2Cl_2, 500 mL of methanol/CH_2Cl_2 (5:95), and 1 L of methanol/CH_2Cl_2 (7.5:92.5) to yield polymer **7** (400 mg, 9%) as a sticky solid. TLC (silica) methanol/CH_2Cl_2 (12.5:87.5) R_f: 0.31. ^{1}H NMR: M_n=1600 Da. ^{1}H NMR (DMSO-d_6): δ 1.37 (s, –CCH_3), 1.58 (m, CH$_2$CH_2CH$_2$), 2.56 (t, NH$_2$CH_2–), 3.40–3.61 (br, –CH$_2$CH_2–, –CH_2CH$_2$O–, and –CH$_2$CH_2O–) ppm.

*4.3.5. Preparation of PAA-g-(CONH–PEG–NH–Boc)-b-PS (**8**): general procedure for amidation of the polymer*

A flame-dried 10 mL round bottom flask equipped with a magnetic stir bar was charged with polymer **5** (100 mg, 8 μmol) and 5 mL of dry DMF. To the stirred solution HOBt (10.8 mg, 80 μmol) and EDCI (15.5 mg, 80 μmol) were added and the reaction was left to proceed for 1 h, after which a solution of polymer **7** (90 mg, 56 μmol, 7 equiv) dissolved in 1 mL of DMF was added. The reaction mixture was further stirred for 20 h at room temperature before being transferred to a presoaked dialysis tubing (MWCO ca. 6000–8000 Da), and dialyzed against nanopure H_2O for 4 days, to remove all of the impurities and afford polymer **8** as a white solid after lyophilization (136 mg, 81%, 5 PEG/polymer chain, 71% coupling efficiency). ^{1}H NMR: M_n=21,000 Da. ^{1}H NMR (DMSO-d_6): δ 0.83 (m, CH_3CH$_2$–), 1.21–1.87 (br, –CHCH_2– of the polymer backbone, alkyl chain of initiator, and HOOCC(CH_3)$_2$–), 1.37 (s, –CCH_3) 2.10–2.41 (br, –CHCH$_2$– of the polymer backbone), 3.41–3.52 (br, –OCH_2CH_2O–), 6.48–7.31 (br, *Ar–H*) ppm.

*4.3.6. Preparation of PAA-g-(CONH–lysine–DOTA–Boc)-b-PS (**9**)*

Polymer **6** (200 mg, 16 μmol), Boc–DOTA–lysine **3** (78.3 mg, 112 μmol, 7 equiv), HOBt (17.3 mg, 128 μmol), and EDCI (24.5 mg, 128 μmol) were allowed to undergo reaction according to the general procedure (Section 4.3.5) outlined for amidation of polymers to yield polymer **9** after dialysis and lyophilization (272 mg, 96%, 5 DOTA–lysine/polymer chain, 71% coupling efficiency). ^{1}H NMR: M_n=17,700 Da. ^{1}H NMR (DMF-d_7): δ 0.86 (m, CH_3CH$_2$–), 1.08 (br, –CH$_2$– of lysine) 1.21–1.87 (br, –CHCH_2– of the polymer backbone, alkyl chain of initiator, and HOOCC(CH_3)$_2$–), 1.47 (s, –CCH_3 DOTA), 2.10–2.41 (br, –CHCH$_2$– of the polymer backbone), 2.45–2.61 and 3.42–4.12 (br, DOTA), 6.49–7.32 (br, *Ar–H*) ppm.

*4.3.7. Preparation of PAA-g-(CONH–lysine–DOTA–Boc)-g-(CONH–PEG–NH–Boc)-b-PS (**10**)*

Polymer **9** (200 mg, 11.3 μmol), polymer **7** (127 mg, 79 μmol, 7 equiv), HOBt (15.3 mg, 113 μmol), and EDCI (21.7 mg, 113 μmol) were allowed to undergo reaction according to the general procedure (Section 4.3.5) outlined for amidation of polymers to yield polymer **10** after dialysis and lyophilization (256 mg, 78%, 4 PEG/polymer chain, 57% coupling efficiency). ^{1}H NMR: M_n=23,900 Da. ^{1}H NMR (DMF-d_7): δ 0.86 (m, CH_3CH$_2$–), 1.08 (br, –CH$_2$– of lysine) 1.21–1.87 (br, –CHCH_2– of the polymer backbone, alkyl chain of initiator, and HOOCC(CH_3)$_2$–), 1.40 (s, –CCH_3 of PEG), 1.47 (s, –CCH_3 DOTA), 2.10–2.41 (br, –CHCH$_2$– of the polymer backbone), 2.45–2.61 and 3.42–4.12 (br, DOTA) and (br, –CH_2CH_2O–), 6.49–7.32 (br, *Ar–H*) ppm.

*4.3.8. Preparation of PAA-g-(CONH–PEG–NH$_2$)-b-PS (**11**)*

Polymer **8** (120 mg, 5.7 μmol) and TFA (3 mL) were allowed to react in CH_2Cl_2 (5 mL) according to the general procedure (Section 4.3.3) outlined for TFA deprotection of polymers to yield polymer **11** after dialysis and lyophilization (85 mg, 72%). ^{1}H NMR: M_n=20,500 Da. ^{1}H NMR (DMSO-d_6): δ 0.83 (m, CH_3CH$_2$–), 1.11–1.97 (br, –CHCH_2– of the polymer backbone, alkyl chain of initiator, and HOOCC(CH_3)$_2$–), 2.10–2.41 (br, –CHCH$_2$– of the polymer backbone), 3.47–3.53 (br, –OCH_2CH_2O–), 6.47–7.25 (br, *Ar–H*) ppm.

*4.3.9. Preparation of PAA-g-(CONH–lysine–DOTA–COOH)-g-(CONH–PEG–NH$_2$)-b-PS (**12**)*

Polymer **10** (220 mg, 9.2 μmol) and TFA (4 mL) were allowed to react in CH_2Cl_2 (6 mL) according to the general procedure (Section 4.3.3) outlined for TFA deprotection of polymers to yield polymer **12** after dialysis and lyophilization (191 mg, 88%). ^{1}H NMR: M_n=23,500 Da. ^{1}H NMR (DMF-d_7): δ 0.88 (m, CH_3CH$_2$–), 1.28 (br, –CH$_2$– of lysine) 1.21–2.00 (br, –CHCH_2– of the polymer backbone, alkyl chain of initiator, and HOOCC(CH_3)$_2$–), 2.10–2.41 (br, –CHCH$_2$– of the polymer backbone), 2.45–2.61 and 3.42–4.12 (br, DOTA) and (br, –CH_2CH_2O–), 6.42–7.41 (br, *Ar–H*) ppm.

*4.3.10. Preparation of PAA-g-(CONH–PEG–NHCO–C$_5$H$_{10}$–SCOCH$_3$)-b-PS (**13**): general procedure for the introduction of masked SH groups*

Polymer **11** (80 mg, 3.9 μmol), and SATH **1** (28 mg, 98 μmol, 5 equiv/NH$_2$) were reacted in dry DMF (5 mL) for 24 h at room temperature before being transferred to a presoaked dialysis tubing (MWCO ca. 6000–8000 Da), and dialyzed against nanopure H_2O for 4 days, to remove all of the impurities and afford polymer **13** as a white solid after lyophilization (68 mg, 82%). ^{1}H NMR: M_n=21,300 Da. ^{1}H NMR (DMSO-d_6): δ 0.83 (m, CH_3CH$_2$–), 1.08–2.01 (br, –CHCH_2– of the polymer backbone, alkyl chain of initiator, and HOOCC(CH_3)$_2$–), 2.15–2.29 (br, –CHCH$_2$– of the polymer backbone), 2.32 (s, –SCOCH_3), 2.71–2.79 (br, –CH$_2$S), 3.47–3.53 (br, –OCH_2-CH_2O–), 6.47–7.25 (br, *Ar–H*) ppm.

*4.3.11. Preparation of PAA-g-(CONH–lysine–DOTA–COOH)-g-(CONH–PEG–NHCO–C_5H_{10}–$SCOCH_3$)-b-PS (**14**)*

Polymer **12** (160 mg, 6.8 μmol), and SATH **1** (49 mg, 170 μmol, 5 equiv/NH_2) were reacted according to the general procedure outlined in Section 4.3.10 to afford polymer **14** as a white solid after lyophilization (158 mg, 95%,). ^{1}H NMR: M_n=24,300 Da. ^{1}H NMR (DMF-d_7): δ 0.84 (m, CH_3CH_2–), 1.10–1.14 (br, –CH_2– of lysine) 1.21–2.00 (br, –CHCH_2– of the polymer backbone, alkyl chain of initiator, and HOOCC(CH_3)$_2$–), 2.10–2.31 (br, –CHCH_2– of the polymer backbone), 2.45–2.61 and 3.38–4.20 (br, DOTA) and (br, –CH_2CH_2O–), 2.72–2.81 (br, –CH_2S), 6.24–7.52 (br, *Ar*–*H*) ppm.

*4.3.12. General procedure for the preparation of the micelles (**15**)*

To a solution of PAA-*g*-(CONH–PEG–NHCO–C_5H_{10}–$SCOCH_3$)-*b*-PS diblock copolymer **13**, in DMF (30 mg, 1.0 mg mL^{-1}), an equal volume of nanopure H_2O was added dropwise via a syringe pump over the course of 3 h. The reaction mixture was further stirred ca. 16 h at room temperature before being transferred to presoaked dialysis tubing (MWCO ca. 6000–8000 Da), and dialyzed against nanopure H_2O for 4 days, to afford a micelle solution **15**, with the final polymer concentration of 0.255 mg mL^{-1}. $(D_h)_n$ (DLS)=21±2 nm; $(D_h)_{vol}$ (DLS)=29±4 nm; D_{av} (TEM)=18±3 nm; H_{av} (AFM)=18±2 nm.

*4.3.13. Preparation of micelle (**16**)*

Polymer **14** was assembled into micelle **16** according to the general procedure (2.3.12), at a final concentration of 0.247 mg mL^{-1}. $(D_h)_n$ (DLS)=25±3 nm; $(D_h)_{vol}$ (DLS)=38±5 nm. Micelle **15** was not stable in solution and precipitated over a course of 10 days, prohibiting accurate AFM and TEM imaging.

*4.3.14. General procedure for the preparation of the SCKs (**17**)*

A solution of 2,2′-(ethylenedioxy)bis(ethylamine) in nanopure H_2O (ca. 1.0 mg mL^{-1}, nominal 50% crosslinking, 6.4 mg, 72 μmol) was added dropwise over 15 min to a solution of micelle **15** in nanopure H_2O (30 mL, 0.255 mg mL^{-1} polymer concentration). The reaction mixture was stirred for ca. 1 h at room temperature. To this solution, a solution of 1-[3′-(dimethylamino)propyl]-3-ethylcarbodiimide methiodide in nanopure H_2O (10.8 mg, 73 μmol) was added dropwise via syringe pump over 15 min. The reaction mixture was further stirred 20 h at room temperature before being transferred to presoaked dialysis tubing (MWCO ca. 6000–8000 Da), and dialyzed against buffer (100 mM PBS, 0.1 M NaCl, 10 mM EDTA, pH 7.4) for 4 days, to remove all of the impurities and afford the SCK solution **17** with a final concentration of 0.249 mg mL^{-1}. $(D_h)_n$ (DLS)=21±5 nm; $(D_h)_{vol}$ (DLS)=29±6 nm; D_{av} (TEM)=16±3 nm; H_{av} (AFM)=14±2 nm.

*4.3.15. General procedure for the deprotection of the SCKs (**18**)*

Hydroxylamine hydrochloride (500 μL, 0.5 M) in aqueous buffer (100 mM PBS, 0.1 M NaCl, 10 mM EDTA, pH 7.4) was added to a stirred solution of 10 mL of SCK **17** suspended in buffer (100 mM PBS, 0.1 M NaCl, 10 mM EDTA, pH 7.4) and stirred for 3 h at room temperature. The solution was assayed by Ellman's method resulting in a concentration of 55±6 μM [HS], theoretical concentration of 58 μM [HS], after which the coupling of maleimido-BSA (mal-BSA) was performed immediately.

*4.3.16. SMCC-modification of tetramethylrhodamine functional BSA (**19**)*

A flame-dried 10 mL vial equipped with a magnetic stir bar was charged with tetramethylrhodamine–BSA (7.2 mg, 0.109 μmol) and 2 mL buffer (100 mM PBS, 0.1 M NaCl, 10 mM EDTA, pH 7.4). To the stirred solution, 200 μL of sulfo-SMCC suspended in DMF (3.57 mg mL^{-1}) was added. The reaction was allowed to proceed for 2 h after which the solution was purified on a Zeba desalting column preconditioned in buffer (100 mM PBS, 0.1 M NaCl, 10 mM EDTA, pH 7.4) and immediately lyophilized to afford maleimido-functionalized BSA 19 (5.28 mg) as a pink solid. The degree of modification was assayed by TNBS, determining that 27% of the NH_2 groups of the BSA had been replaced by maleimido groups. $(D_h)_n$ (DLS)=2.2±0.7 nm; $(D_h)_{vol}$ (DLS)=2.3±0.1 nm.

*4.3.17. General procedure for the functionalization of the SCK with BSA (**20**)*

BSA-maleimide (300 μL, 1.65 mg mL^{-1}, 10 equiv per SCK) suspended in buffer (100 mM PBS, 0.1 M NaCl, 10 mM EDTA, pH 7.4) was added to a stirred solution of SCK **19** (10 mL, 0.249 mg mL^{-1}) suspended in buffer (100 mM PBS, 0.1 M NaCl, 10 mM EDTA, pH 7.4). The reaction was allowed to proceed for 6 h, after which the reaction was quenched by the addition of *N*-ethyl maleimide (0.77 mg, 10 equiv per SH group suspended in DMSO). The solution was thereafter stirred for 16 h before being transferred to presoaked dialysis tubing (MWCO ca. 100 kDa), and dialyzed against buffer (5 mM PBS, 5 mM NaCl, pH 7.4) for 7 days, to remove unconjugated BSA and small molecule impurities and afford the pink SCK solution **20**. $(D_h)_n$ (DLS)=31±3 nm; $(D_h)_{vol}$ (DLS)=50±7 nm (bimodal); D_{av} (TEM)=20±2 nm. BSA determination by Commassie (Bradford) assay resulted in a BSA concentration of 20±8 μg mL^{-1}; theoretical BSA concentration of 32 μg mL^{-1}. BSA determination by UV–vis spectroscopy (550 nm tetramethylrhodamine) gave a concentration of ~6 μg mL^{-1} (below accurate calibration); theoretical BSA concentration of 32 μg mL^{-1}.

*4.3.18. BSA conjugation (**21**)*

BSA-maleimide (600 μL, 1.65 mg mL^{-1}, 20 equiv per SCK) and SCK **18** (10 mL, 0.249 mg mL^{-1}) were reacted according to the general procedure outlined in Section 4.3.17 to afford SCK **21**. $(D_h)_n$ (DLS)=32±5 nm; $(D_h)_{vol}$ (DLS)=47±6 nm (bimodal); D_{av} (TEM)=20±3 nm. BSA determination by Commassie (Bradford) assay resulted in a BSA concentration of 37±8 μg mL^{-1}; theoretical BSA concentration of 64 μg mL^{-1}. BSA determination by UV–vis spectroscopy (550 nm tetramethylrhodamine) gave a concentration of 43 μg mL^{-1}; theoretical BSA concentration of 64 μg mL^{-1}.

*4.3.19. BSA conjugation (**22**)*

BSA-maleimide (903 μL, 1.65 mg mL^{-1}, 30 equiv per SCK) and SCK **18** (10 mL, 0.249 mg mL^{-1}) were reacted according to the general procedure outlined in Section 4.3.17 to afford SCK **22**. $(D_h)_n$ (DLS)=28±3 nm; $(D_h)_{vol}$ (DLS)=42±4 nm (bimodal); D_{av} (TEM)=20±3 nm. BSA determination by Commassie (Bradford) assay resulted in a BSA concentration of 85±8 μg mL^{-1}; theoretical BSA concentration of 119 μg mL^{-1}. BSA determination by UV–vis spectroscopy (550 nm tetramethylrhodamine) gave a concentration of 81 μg mL^{-1}; theoretical BSA concentration of 119 μg mL^{-1}.

Acknowledgements

This material is based upon work supported by the National Heart Lung and Blood Institute of the National Institutes of Health as a Program of Excellence in Nanotechnology (HL080729). Postdoctoral and assistant professor fellowship provided by the Knut and Alice Wallenberg Foundation is gratefully acknowledged (A.M.N). The authors thank Mr. G.M. Veith for TEM imaging.

Supplementary data

Supplementary data associated with this article can be found in the online version, at doi:10.1016/j.tet.2008.04.104.

References and notes

1. Allen, T. M.; Cullis, P. R. *Science* **2004**, *303*, 1818–1822.
2. Duncan, R. *Nat. Rev. Drug Discov.* **2003**, *2*, 347–360.
3. Ferrari, M. *Nat. Rev. Cancer* **2005**, *5*, 161–171.
4. Langer, R. *Nature* **1998**, *392*, 5–10.
5. Weissleder, R.; Kelly, K.; Sun, E. Y.; Shtatland, T.; Josephson, L. *Nat. Biotechnol.* **2005**, *23*, 1418–1423.
6. Gref, R.; Minamitake, Y.; Peracchia, M. T.; Trubetskoy, V.; Torchilin, V.; Langer, R. *Science* **1994**, *263*, 1600–1603.
7. Nahar, M.; Dutta, T.; Murugesan, S.; Asthana, A.; Mishra, D.; Rajkumar, V.; Tare, M.; Saraf, S.; Jain, N. K. *Crit. Rev. Ther. Drug Carrier Syst.* **2006**, *23*, 259–318.
8. Li, Y.; Sun, G.; Xu, J.; Wooley, K. L. *Nanotechnol. Ther.* **2007**, 381–407.
9. O'Reilly, R. K.; Hawker, C. J.; Wooley, K. L. *Chem. Soc. Rev.* **2006**, *35*, 1068–1083.
10. O'Reilly, R. K.; Joralemon, M. J.; Hawker, C. J.; Wooley, K. L. *J. Polym. Sci., Part A: Polym. Chem.* **2006**, *44*, 5203–5217.
11. Thurmond, K. B.; Kowalewski, T.; Wooley, K. L. *J. Am. Chem. Soc.* **1996**, *118*, 7239–7240.
12. Thurmond, K. B.; Kowalewski, T.; Wooley, K. L. *J. Am. Chem. Soc.* **1997**, *119*, 6656–6665.
13. Read, E. S.; Armes, S. P. *Chem. Commun.* **2007**, 3021–3035.
14. Becker, M. L.; Liu, J.; Wooley, K. L. *Chem. Commun.* **2003**, 180–181.
15. Liu, J.; Zhang, Q.; Remsen, E. E.; Wooley, K. L. *Biomacromolecules* **2001**, *2*, 362–368.
16. Sun, G.; Hagooly, A.; Xu, J.; Nyström, A. M.; Li, Z.; Rossin, R.; Moore Dennis A.; Wooley, K. L.; Welch, M. J, submitted for publication.
17. Sun, G.; Xu, J.; Hagooly, A.; Rossin, R.; Li, Z.; Moore, D. A.; Hawker, C. J.; Welch, M. J.; Wooley, K. L. *Adv. Mater.* **2007**, *19*, 3157–3162.
18. Turner, J. L.; Becker, M. L.; Li, X.; Taylor, J.-S. A.; Wooley, K. L. *Soft Matter* **2005**, *1*, 69–78.
19. Turner, J. L.; Pan, D.; Plummer, R.; Chen, Z.; Whittaker, A. K.; Wooley, K. L. *Adv. Funct. Mater.* **2005**, *15*, 1248–1254.
20. Xu, J.; Sun, G.; Rossin, R.; Hagooly, A.; Li, Z.; Fukukawa, K.-I.; Messmore, B. W.; Moore, D. A.; Welch, M. J.; Hawker, C. J.; Wooley, K. L. *Macromolecules* **2007**, *40*, 2971–2973.
21. Harris, L. J.; Larson, S. B.; Hasel, K. W.; Day, J.; Greenwood, A.; McPherson, A. *Nature* **1992**, *360*, 369–372.
22. Nyström, A. M.; Wooley, K. L., unpublished results.
23. Roberts, M. J.; Bentley, M. D.; Harris, J. M. *Adv. Drug Deliv. Rev.* **2002**, *54*, 459–476.
24. Pressly, E. D.; Rossin, R.; Hagooly, A.; Fukukawa, K.-I.; Messmore, B. W.; Welch, M. J.; Wooley, K. L.; Lamm, M. S.; Hule, R. A.; Pochan, D. J.; Hawker, C. J. *Biomacromolecules* **2007**, *8*, 3126–3134.
25. Klaikherd, A.; Ghosh, S.; Thayumanavan, S. *Macromolecules* **2007**, *40*, 8518–8520.
26. Ghosh, S.; Basu, S.; Thayumanavan, S. *Macromolecules* **2006**, *39*, 5595–5597.
27. Allen, T. M.; Brandeis, E.; Hansen, C. B.; Kao, G. Y.; Zalipsky, S. *Biochim. Biophys. Acta* **1995**, *1237*, 99–108.
28. Beduneau, A.; Saulnier, P.; Hindre, F.; Clavreul, A.; Leroux, J.-C.; Benoit, J.-P. *Biomaterials* **2007**, *28*, 4978–4990.
29. Dufresne, M.-H.; Gauthier, M. A.; Leroux, J.-C. *Bioconjugate Chem.* **2005**, *16*, 1027–1033.
30. *Bioconjugate Techniques*; Hermanson, G. T., Ed.; Academic: San Diego, CA, 1996.
31. Kakizawa, Y.; Harada, A.; Kataoka, K. *J. Am. Chem. Soc.* **1999**, *121*, 11247–11248.
32. *Adoptive Immunotherapy: Methods and Protocols*; Ludewig, B., Hoffmann, M. W., Eds.; Methods in Molecular Medicine; Humana: 2005; Vol. 109.
33. Tong, R.; Cheng, J. *Polym. Rev.* **2007**, *47*, 345–381.
34. Tsarevsky, N. V.; Matyjaszewski, K. *Macromolecules* **2005**, *38*, 3087–3092.
35. van Dijk-Wolthuis, W. N. E.; Van de Wetering, P.; Hinrichs, W. L. J.; Hofmeyer, L. J. F.; Liskamp, R. M. J.; Crommelin, D. J. A.; Hennink, W. E. *Bioconjugate Chem.* **1999**, *10*, 687–692.
36. Carrillo, A.; Yanjarappa, M. J.; Gujraty, K. V.; Kane, R. S. *J. Polym. Sci., Part A: Polym. Chem.* **2005**, *44*, 928–939.
37. Shukla, R.; Thomas, T. P.; Peters, J. L.; Desai, A. M.; Kukowska-Latallo, J.; Patri, A. K.; Kotlyar, A.; Baker, J. R., Jr. *Bioconjugate Chem.* **2006**, *17*, 1109–1115.
38. Shi, M.; Wosnick, J. H.; Ho, K.; Keating, A.; Shoichet, M. S. *Angew. Chem., Int. Ed.* **2007**, *46*, 6126–6131.
39. Shechter, Y.; Mironchik, M.; Saul, A.; Gershonov, E.; Precido-Patt, L.; Sasson, K.; Tsubery, H.; Mester, B.; Kapitkovsky, A.; Rubinraut, S.; Vachutinski, Y.; Fridkin, G.; Fridkin, M. *Int. J. Pept. Protein Res.* **2007**, *13*, 105–117.
40. Ellman, G. L. *Arch. Biochem. Biophys.* **1959**, *82*, 70–77.
41. Adrian, J. E.; Kamps, J. A. A. M.; Scherphof, G. L.; Meijer, D. K. F.; van Loenen-Weemaes, A.-M.; Reker-Smit, C.; Terpstra, P.; Poelstra, K. *Biochim. Biophys. Acta* **2007**, *1768*, 1430–1439.
42. Bradford, M. M. *Anal. Biochem.* **1976**, *72*, 248–254.
43. Liu, L.; Rozenman, M.; Breslow, R. *J. Am. Chem. Soc.* **2002**, *124*, 12660–12661.
44. Lai, J. T.; Filla, D.; Shea, R. *Macromolecules* **2002**, *35*, 6754–6756.
45. Habeeb, A. F. S. A. *Anal. Biochem.* **1966**, *14*, 328–336.
46. Sashidhar, R. B.; Capoor, A. K.; Ramana, D. *J. Immunol. Methods* **1994**, *167*, 121–127.